Earthq Eng & Eng Vib (2021) 20: 993-1006 **DOI**: https://doi.org/10.1007/s11803-021-2064-1

Conventional vs. modified pseudo-dynamic seismic analyses in the shallow strip footing bearing capacity problem

Ghazal Rezaie Soufi[1†], Reza Jamshidi Chenari[1‡] and Sina Javankhoshdel[2§]

1. *Department of Civil Engineering, Faculty of Engineering, University of Guilan, P.O. 3756, Rasht, Guilan, Iran*

2. *Rocscience Inc., 54 Saint Patrick St., Toronto M5T 1V1, Ontario, Canada*

Abstract: The conventional pseudo-dynamic (CPD) and modified pseudo-dynamic (MPD) methods are invoked to obtain the seismic bearing capacity of strip foundations using the limit equilibrium method, with a two-wedge failure mechanism. A spectral version of the conventional pseudo-dynamic method (SPD) is also invoked by considering the ground motion amplification factor, to be a function of the non-dimensional frequency λ/B and soil damping. Numeric analyses show that bearing capacity results obtained by the MPD and SPD methods are generally consistent. Both experience the same general reduction in bearing capacity with the increase of λ/B, with successive ups and downs corresponding to soil's natural frequencies. For $5<\lambda/B<10$, SPD and MPD results fluctuated between falling above and below CPD results. For $\lambda/B<2.5$, SPD and MPD results were consistent with attenuation of the shear wave, while for $10<\lambda/B$, amplification was exhibited. Results obtained by the CPD method monotonically decrease, due to the fact that CPD fails to inherently consider site effects and damping, and instead and relies on a single factor to consider the ground motion amplification.

Keywords: bearing capacity; modified pseudo-dynamic method; conventional pseudo-dynamic method; spectral analysis

1 Introduction

The pseudo-static and pseudo-dynamic methods are among the most commonly-used approaches in seismic stability analysis, including investigating the seismic bearing capacity of shallow foundations. Although simple and robust, the pseudo-static method subjects the entire soil mass to the same acceleration and assumes the magnitude and phase of the accelerations to be invariant through the soil body, essentially failing to consider the effects of time duration, phase differences and frequency contents on the bearing capacity of shallow footings. The pseudo-dynamic method, developed by Steedman and Zeng (1990) to investigate seismic lateral stresses on a retaining wall, is able to take into account phase differences in the acceleration, and consider amplification in the soil body. The pseudo-dynamic method was later improved upon by Choudhury and Nimbalkar (2005, 2006) to include the effect of both primary and shear waves on the lateral stresses on a vertical retaining wall. In addition to being used by many researchers to calculate the lateral stresses on retaining walls (Choudhury *et al*., 2007; Nimbalkar and Choudhury, 2007, 2008; Ghosh, 2007, 2008a, 2010; Azad *et al*., 2008; Shafiee *et al*., 2010; Wang *et al*., 2011; Ghosh and Kolathayar, 2011; Ruan *et al*., 2012; Ghosh and Sharma, 2012; Ruan *et al*., 2013a; Ghosh and Saha, 2014; Fathipour *et al*., 2021a, 2021b), the method has since been further upgraded to apply to different problems including seismic displacement in walls (Choudhury and Nimbalkar, 2007, 2008; Basha and Babu, 2009b, 2010, 2011), nonvertical walls (Ghanbari and Ahmadabadi, 2010), retaining walls with submerged backfills (Choudhury and Ahmad, 2008; Ahmad and Choudhury, 2008b, 2010; Bellezza *et al*., 2012; Chakraborty and Choudhury, 2014a, 2014b; Rajesh and Choudhury, 2017a, 2017b), reinforced soil walls (Nimbalkar *et al*., 2006; Ahmad and Choudhury, 2008a; Shekarian *et al*., 2008; Shekarian and Ghanbari, 2008; Basha and Babu, 2009a; Narasimha Reddy *et al*., 2009; Cheng *et al*., 2013; Ruan and Sun, 2013; Ruan *et al*., 2018). In addition, the pseudo-dynamic method has been effectively used to investigate the seismic stability of slopes (Eskandarinejad and Shafiee, 2011; Ruan *et al*., 2013b; Qin and Chian, 2018), vertical excavations (Sarangi and Ghosh, 2016; Pain *et al*., 2017a) and landslides (Zhou *et al*., 2015) and finally to determine the seismic bearing capacity of shallow foundations (Ghosh, 2008b; Ghosh and Choudhury, 2011; Saha and Ghosh 2015a, 2015b; Zhou *et al*., 2016; Saha *et al*., 2018; Kurup and Kolathayar, 2018; Izadi *et al*., 2019; Safardoost Siahmazgi *et al*., 2021).

Despite being an improvement over the pseudo-

Correspondence to: Reza Jamshidi Chenari, Department of Civil Engineering, Faculty of Engineering, University of Guilan, P.O. 3756, Rasht, Guilan, Iran
Tel: +98-13-33690485; Fax: +98-13-33690485
E-mail: Jamshidi_reza@guilan.ac.ir
†PhD Candidate; ‡Associate Professor; §Geomechanics Specialist
Received June 6, 2020; **Accepted** February 17, 2021

static approach, the pseudo-dynamic approach is not without its own flaws. Bellezza (2014), Choudhury *et al*. (2014) and Pain *et al*. (2015) criticized the pseudo-dynamic method for failing to satisfy the traction-free boundary condition at the surface, for assuming a linear variation profile of the acceleration amplification along the soil depth, and requiring an a priori assumption on the amplification factor, while also neglecting to take the soil′s damping characteristics into account. Bellezza (2014) clarified that the pseudo-dynamic method failed to take account of reflection at the soil′s free surface and thereby, the waves modeled in this method are merely incident waves travelling upward through a linear elastic backfill, which results in the violation of the zero-stress boundary at the surface. Bellezza (2014, 2015) developed an improved pseudo-dynamic method where the soil was modeled as a visco-elastic Kelvin-Voigt material instead of a linear elastic material, in order to include the effects of soil′s damping properties. By modeling the shear and compression waves as standing waves, Bellezza (2014, 2015) managed to include the interference of the upward and downward travelling waves generated as a result of reflection. Through this method, the travelling waves are inherently amplified in the soil stratum without the need of applying an extra amplification factor. This modified pseudo-dynamic method was later used by Pain *et al*. (2015), Pain *et al*. (2017b), Rajesh and Choudhury (2017) and Khatri (2019) to investigate the lateral stresses and stability of retaining walls, and by Pain *et al*. (2016a) to determine the uplift capacity of horizontal strip anchors. In addition, the modified pseudo-dynamic method has been used by Pain *et al*. (2016a, b), Nadgouda and Choudhury (2019) and Saha and Ghosh (2020) to investigate the bearing capacity of shallow foundations.

In this study, the conventional and modified pseudo-dynamic approaches are compared in their ability to predict the seismic bearing capacity of strip foundations, using the limit equilibrium method with a simple two-wedge failure mechanism, also known as the Coulomb mechanism. The two-wedged mechanism, developed as a useful simplification to the Prandtl (1921) failure surface, was used by Richards *et al*. (1993) in their investigation into the seismic bearing capacity and settlement of foundations. It has since been used by different researchers (Ghosh, 2008; Saha and Ghosh, 2015; Pain *et al*., 2016; Ghosh and Debnath, 2017; Saha and Ghosh, 2017; Izadi *et al*., 2019) in their investigations of seismic bearing capacity, thanks to its simplicity. In addition to the pseudo-dynamic methods, static and pseudo-static (PS) bearing capacity factors, have been calculated for the presented mechanism and are included in the results for comparison. Moreover, extra pseudo-dynamic analyses are conducted with the amplification factor, introduced as a function of damping and wavelength and these analyses are referred to as the spectral pseudo-dynamic method (SPD). It must be noted that by this title, it is not meant to say that the other two methods are not spectral, since all pseudo-dynamic methods are frequency-dependent and spectral. The title "spectral" refers to the modification of the conventional pseudo-dynamic method to a method that includes a spectral amplification analysis.

2 Method

2.1 Pseudo-dynamic formulations

Equation (1) presents the horizontal pseudo-dynamic acceleration function for a sinusoidal base shaking, at any depth z below the surface, at the time t, as proposed by Steedman and Zeng (1990).

$$\begin{aligned} a_h(z,t) &= k_{\mathrm{h,base}}\mathrm{g}\xi \\ &= k_{\mathrm{h,base}}\mathrm{g}\left[1+\frac{H-z}{H}(f_{\mathrm{a}}-1)\right]\sin\omega\left(t-\frac{H-z}{V_{\mathrm{s}}}\right) \end{aligned} \tag{1}$$

where a_{h} is the horizontal acceleration at any depth z below the footing base at the time t, ξ represents the oscillation factor, ω is the angular frequency, $k_{\mathrm{h,base}}$ is the horizontal coefficient of acceleration at the base level, g is the gravitational acceleration, f_{a} is the amplification factor, H is the soil depth over the bedrock and V_{s} is the shear wave velocity. While soil shear wave velocity is usually a spatially variable parameter (Kazemi Esfeh *et al*., 2020), as per Steedman and Zeng (1990), the shear wave velocity is assumed to be constant along the soil depth. In Eq. (1), both the effects of phase differences as well as changes in the magnitude of acceleration along the height (amplification or attenuation) are considered. The term $\sin(\omega \times (t - (H - z) / V_{\mathrm{s}}))$ applies the phase differences to the acceleration function based on time and depth. In this term, the normalized frequency, $\omega H/V_{\mathrm{s}}$ is an important parameter that is proportional to the time it takes for the wave to travel upward to the surface (H/V_{s}) normalized to the period of the base shaking. $\omega H/V_{\mathrm{s}}$ is inversely proportional to the normalized shear wavelength or λ/H where λ is the shear wavelength. These factors implement the effect of the earthquake frequency, as well as the dynamic properties of the soil into the acceleration function. In addition, when the shear wave travels upward from the base towards the surface, depending on the site effects, damping and depth of the soil, the magnitude of the acceleration can be magnified. In Eq. (1), the term $(1 + (H - z) \times (f_{\mathrm{a}} - 1) / H)$ applies the effects of amplification to the acceleration function. Based on this factor, the f_{a} is assumed a constant and the acceleration magnitude varies linearly along the soil depth. By taking into account the effects of phase differences, excitation frequency and amplification, the pseudo-dynamic analysis delivers results that differ from the pseudo-static and static bearing capacities depending on the seismic wavelength.

Equation (2) presents the horizontal modified pseudo-dynamic acceleration function for a sinusoidal base shaking, at any depth z below the surface, at the time t.

$$a_{\mathrm{h}}(z,t)=k_{\mathrm{h,base}}\mathrm{g}\xi=$$
$$\frac{k_{\mathrm{h,base}}\mathrm{g}}{C^2+S^2}[(CC_z+SS_z)\cos(\omega t)+(SC_z-CS_z)\sin(\omega t)] \quad (2)$$

where

$$C=\cos(y_1)\cosh(y_2) \qquad S=-\sin(y_1)\sinh(y_2)$$

$$C_z=\cos(\frac{y_1 z}{H})\cosh(\frac{y_2 z}{H}) \qquad S_z=-\sin(\frac{y_1 z}{H})\sinh(\frac{y_2 z}{H})$$

$$y_1=\frac{\omega H}{V_{\mathrm{s}}}\sqrt{\frac{\sqrt{(1+4D^2)}+1}{2(1+4D^2)}} \quad y_2=-\frac{\omega H}{V_{\mathrm{s}}}\sqrt{\frac{\sqrt{(1+4D^2)}-1}{2(1+4D^2)}}$$

where D is the soil damping ratio. As previously mentioned, a major criticism of the conventional pseudo-dynamic method (CPD) is aimed at its inability to take into account the damping properties of the soil. As an alternative the amplification factor f_{a}, function in the conventional method can be introduced as a function of the wavelength and damping. This can be done by using the amplification function obtained in a one-dimensional ground response analysis of soil, in the modified pseudo-dynamic method (MPD). The amplification function in this case is the magnitude of the transfer function obtained from the one-dimensional ground response analysis of soil as a Kelvin-Voigt solid, as carried out by Bellezza (2014) and presented by Kramer (1996). The transfer function is defined as the ratio of the amplitudes at the surface and the base rock bottom. Kramer (1996) presented the aforesaid amplification function according to Eq. (3), for the one-dimensional ground response analysis of a uniform soil layer of damping ratio D, characterized as a Kelvin-Voigt solid, placed over a rigid bedrock.

$$F=\frac{1}{\sqrt{\cos^2(2\pi(H/\lambda))+\left(2\pi D(H/\lambda)\right)^2}} \quad (3)$$

where F is the amplification function. By adopting this amplification function as the amplification factor, f_{a}, the conventional pseudo-dynamic method can be elevated to operate as a spectral analysis that also takes into consideration soils′ damping properties.

2.2 Problem definition

A strip footing of width B is placed at a depth of D_{f}, over a soil deposit with the unit weight of γ, friction angle, φ, and cohesion, c, with an underlying semi-infinite bedrock layer, located at a depth of H to the footing. Figure 1 presents a schematic view of the problem under study. The limit equilibrium method with the simplified two-wedge Coulomb failure mechanism is adopted for the bearing capacity analyses. α and β are the inclination angles of the active and passive zones, respectively. h is the depth of the failure mechanism, P_L is the foundation load, Q_{hA} is the inertia force of the active wedge, Q_{hP} is the inertia force on the passive wedge, Q is the overburden load, Q_{hQ} is the inertia force on the surcharge soil block, W_A is the weight of the active wedge, W_P is the weight of the passive wedge, C_{LN} is the cohesive load on the LN surface, C_{NO} is the cohesive load on the NO surface, R_A is the active earth pressure and R_P is the passive earth pressure.

Shear wave velocity was assumed to be constant throughout the soil deposit. Jamshidi Chenari and Aminzadeh Bostani Taleshani (2016) illustrated that the adoption of a proper averaging scenario will yield equivalent homogenous conditions, rendering consistent site response amplification regimes. This has lent support to the contention of constant equivalent shear wave velocity in soil deposits overlying the rigid bedrock hemisphere. The seismic forces induced by the conventional and modified pseudo-dynamic methods are calculated by defining the mass of the thin elements in the active and passive wedges and the surcharge soil block overlying the passive wedge according to Eq. (4). In the conventional pseudo-dynamic method, these elements are subjected to the acceleration field defined by Eq. (1), while for the modified pseudo-dynamic formulation, the acceleration field is defined by Eq. (2).

$$\begin{aligned}
\mathrm{d}m(z)_{\mathrm{A}}&=\frac{\gamma_{\mathrm{e}}(h-z)}{\mathrm{g}\tan\alpha}\mathrm{d}z\\
\mathrm{d}m(z)_{\mathrm{P}}&=\frac{\gamma(h-z)}{\mathrm{g}\tan\beta}\mathrm{d}z\\
\mathrm{d}m(z)_{\mathrm{Q}}&=\frac{\gamma B\tan\alpha}{\mathrm{g}\tan\beta}\mathrm{d}z
\end{aligned} \quad (4)$$

where $\mathrm{d}m(z)_A$, is the mass of a thin element in the active wedge, $\mathrm{d}m(z)_P$ is the mass of a thin element in the passive wedge, and $\mathrm{d}m(z)_Q$ is the mass of thin element in the surcharge soil block at the depth of z. γ_{e} is the equivalent

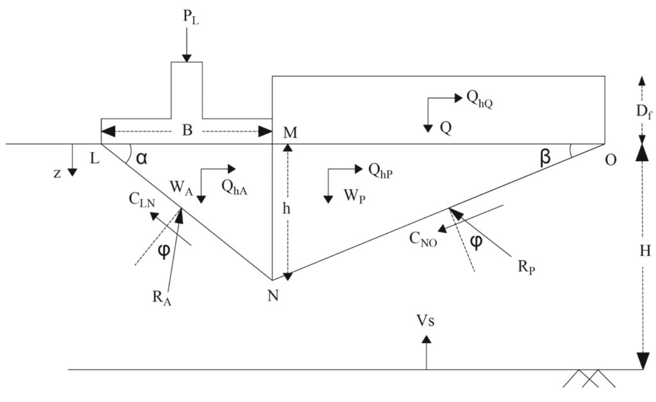

Fig. 1 Problem definition and failure mechanism

soil unit weight for the active wedge, taking into account both the unit weight of the soil and the load applied by the overlying superstructure at the foundation base level. The equivalent unit weight (γ_e) can be found according to Eq. (5).

$$\gamma_e = \gamma + \frac{2P_L}{B^2 \tan\alpha} \tag{5}$$

The horizontal inertia forces acting on the active and passive wedges and the surcharge soil block obtained adopting the conventional pseudo-dynamic method can be found according to Eqs. (6), (7) and (8).

$$Q_{hA,CPD} = \int_0^h a_h(z,t)\mathrm{d}m(z)_A = \frac{\gamma_e k_h B\lambda}{4\pi^3 \tan\alpha}\left[\begin{array}{l} \left((1-f_a)\dfrac{\lambda^2}{BH} + 2\pi^2 f_a \tan\alpha\right)\cos\left(2\pi(\dfrac{H}{\lambda}-\dfrac{t}{T})\right) \\ -(1-f_a)\dfrac{\lambda^2}{BH}\cos\left(2\pi(\dfrac{H}{\lambda}-\dfrac{B}{\lambda}\tan\alpha-\dfrac{t}{T})\right) \\ +\pi\left((1-f_a)\dfrac{\lambda}{H}\tan\alpha - \dfrac{\lambda}{B}f_a\right)\sin\left(2\pi(\dfrac{H}{\lambda}-\dfrac{t}{T})\right) \\ +\pi\left((1-f_a)\dfrac{\lambda}{H}\tan\alpha + \dfrac{\lambda}{H}f_a\right)\sin\left(2\pi(\dfrac{H}{\lambda}-\dfrac{B}{\lambda}\tan\alpha-\dfrac{t}{T})\right) \end{array}\right] \tag{6}$$

where $Q_{hA,CPD}$ is the inertia force of the active wedge according to the conventional pseudo-dynamic method and T is the wave period.

$$Q_{hP,CPD} = \int_0^h a_h(z,t)\mathrm{d}m(z)_P = \frac{\gamma k_h B\lambda}{4\pi^3 \tan\beta}\left[\begin{array}{l} \left((1-f_a)\dfrac{\lambda^2}{BH} + 2\pi^2 f_a \tan\alpha\right)\cos\left(2\pi(\dfrac{H}{\lambda}-\dfrac{t}{T})\right) \\ -(1-f_a)\dfrac{\lambda^2}{BH}\cos\left(2\pi(\dfrac{H}{\lambda}-\dfrac{B}{\lambda}\tan\alpha-\dfrac{t}{T})\right) \\ +\pi\left((1-f_a)\dfrac{\lambda}{H}\tan\alpha - \dfrac{\lambda}{B}f_a\right)\sin\left(2\pi(\dfrac{H}{\lambda}-\dfrac{t}{T})\right) \\ +\pi\left((1-f_a)\dfrac{\lambda}{H}\tan\alpha + \dfrac{\lambda}{H}f_a\right)\sin\left(2\pi(\dfrac{H}{\lambda}-\dfrac{B}{\lambda}\tan\alpha-\dfrac{t}{T})\right) \end{array}\right] \tag{7}$$

where $Q_{hP,CPD}$ is the inertia force on the passive wedge according to the conventional pseudo-dynamic method.

$$Q_{hQ,CPD} = \int_0^{D_f} a_h(z,t)\mathrm{d}m(z)_Q = \frac{\gamma\lambda B k_h \cos\beta\sin\alpha}{2\pi\cos\alpha\sin\beta}\left[\begin{array}{l} (f_a-1)\left[\begin{array}{l} \dfrac{\lambda}{2\pi H}\left[\begin{array}{l}\sin\left(2\pi(\dfrac{t}{T}+\dfrac{D_f}{\lambda}-\dfrac{H}{\lambda})\right) \\ -\sin\left(2\pi(\dfrac{t}{T}-\dfrac{H}{\lambda})\right)\end{array}\right] \\ -\dfrac{D_f}{H}\cos\left(2\pi(\dfrac{t}{T}+\dfrac{D_f}{\lambda}-\dfrac{H}{\lambda})\right) \end{array}\right] + \\ f_a\left(\cos\left(2\pi(\dfrac{t}{T}-\dfrac{H}{\lambda})\right) - \cos\left(2\pi(\dfrac{t}{T}+\dfrac{D_f}{\lambda}-\dfrac{H}{\lambda})\right)\right) \end{array}\right] \tag{8}$$

where $Q_{hQ,CPD}$ is the inertia force on the surcharge soil block according to the conventional pseudo-dynamic method.

Switching to the modified pseudo-dynamic method, the horizontal inertia forces acting on the active and passive wedges and the surcharge soil block can be found according to Eqs. (9), (10) and (11).

$$Q_{hA,MPD} = \int_0^h a_h(z,t)\mathrm{d}m(z)_A = \int_0^h \frac{k_h\gamma_e}{C^2+S^2}\cdot [(CC_z+SS_z)\cos(\omega t)+(SC_z-CS_z)\sin(\omega t)]\frac{(h-z)}{\tan\alpha}\mathrm{d}z \tag{9}$$

$$Q_{hP,MPD} = \int_0^h a_h(z,t)\mathrm{d}m(z)_P = \int_0^h \frac{k_h\gamma}{C^2+S^2}\cdot [(CC_z+SS_z)\cos(\omega t)+(SC_z-CS_z)\sin(\omega t)]\frac{(h-z)}{\tan\beta}\mathrm{d}z \tag{10}$$

$$Q_{hQ,MPD} = \int_0^{D_f} a_h(z,t)\mathrm{d}m(z)_Q = \int_0^{D_f} \frac{k_h\gamma B}{C^2+S^2}\cdot [(CC_z+SS_z)\cos(\omega t)+(SC_z-CS_z)\sin(\omega t)]\frac{(h-z)\tan\alpha}{\tan\beta}\mathrm{d}z \tag{11}$$

where $Q_{hA,\,MPD}$ is the inertia force of the active wedge, $Q_{hP,\,MPD}$ is the inertia force on the passive wedge and $Q_{hQ,\,MPD}$ is the inertia force on the surcharge soil block according to the modified pseudo-dynamic method.

The horizontal inertia forces acting on the active and passive wedges and the surcharge soil block obtained adopting the pseudo-static method can be found according to Eqs. (12), (13) and (14).

$$Q_{hA,PS} = \frac{k_h}{2}\gamma_e B^2\tan\alpha \tag{12}$$

$$Q_{hP,PS} = \frac{k_h}{2}\gamma B^2\frac{\tan^2\alpha}{\tan\beta} \tag{13}$$

$$Q_{hQ,PS} = \frac{k_h}{2}\gamma B D_f\frac{\tan\alpha}{\tan\beta} \tag{14}$$

where $Q_{hA,PS}$ is the inertia force of the active wedge, $Q_{hP,PS}$ is the inertia force on the passive wedge and $Q_{hQ,PS}$ is the inertia force on the surcharge soil block according to the pseudo-static method. Figure 2 shows the forces acting on the active and passive wedges. C_{MN} is the cohesive force on the MN surface. P_A is the active thrust pushing the adjacent passive zone and P_P is the passive thrust,

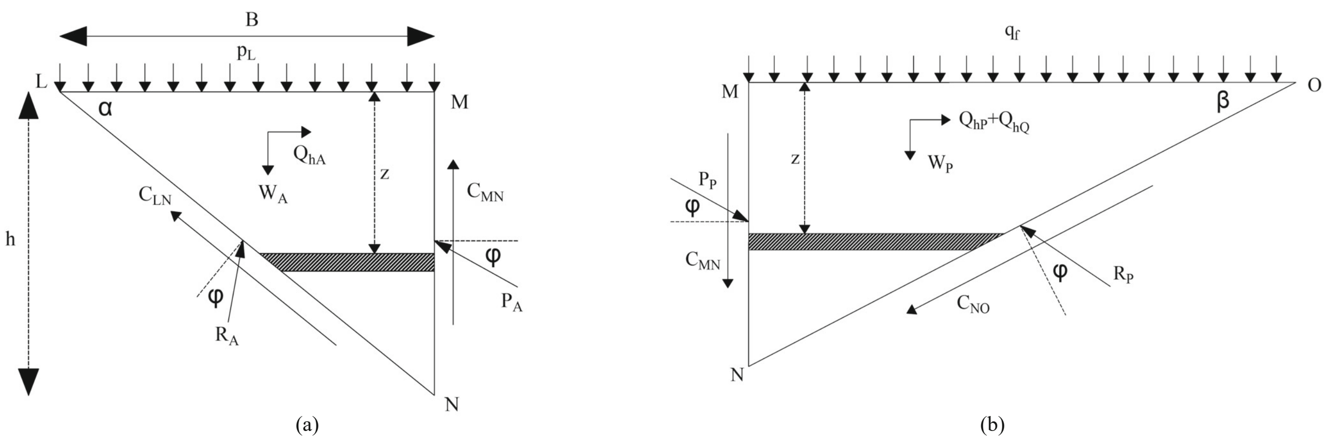

Fig. 2 Forces acting on the failure wedges; a) active zone; b) passive zone

resisting the active wedge. The active and passive lateral earth pressures are equated to satisfy equilibrium.

Equilibrium enforces the Eqs. (15) and (16) on the forces applied to the active wedge:

$$P_A \cos\varphi = R_A \sin(\alpha-\varphi) + Q_{hA} - cB \tag{15}$$

$$P_A \sin\varphi = -R_A \cos(\alpha-\varphi) + W_A - 2cB\tan\alpha + P_L \tag{16}$$

Therefore:

$$P_A = \frac{1}{\cos(\alpha-2\varphi)} \cdot \begin{Bmatrix} Q_{hA}\cos(\alpha-\varphi) + W_A\sin(\alpha-\varphi) - cB\cos(\alpha-\varphi) \\ -2cB\tan\alpha\sin(\alpha-\varphi) + p_L B\sin(\alpha-\varphi) \end{Bmatrix} \tag{17}$$

W_A is defined by Eq. (18):

$$W_A = \frac{1}{2}\gamma B^2 \tan\alpha \tag{18}$$

Similarly, equilibrium conditions enforce Eqs. (19) and (20) on the forces applied to the passive wedge:

$$P_p \sin\varphi = R_p\cos(\beta+\varphi) - W_p - 2cB\tan\varphi - Q \tag{19}$$

$$P_p \cos\varphi = R_p\sin(\beta+\varphi) - Q_{hP} - Q_{hQ} + cB\frac{\tan\alpha}{\tan\beta} \tag{20}$$

W_p is defined according to Eq. (21):

$$W_P = \frac{\gamma}{2}\frac{B^2\tan^2\alpha}{\tan\beta} \tag{21}$$

Q is defined by Eq. (22):

$$Q = q_{\mathrm{f}} B\frac{\tan\alpha}{\tan\beta} = D_{\mathrm{f}}\gamma B\frac{\tan\alpha}{\tan\beta} \tag{22}$$

where q_{f} is the overburden pressure.

Therefore:

$$P_p = \frac{1}{\cos(\beta+2\varphi)} \cdot \begin{Bmatrix} (-Q_{hP} - Q_{hQ})\cos(\beta+\varphi) + (W_p+Q)\sin(\beta+\varphi) \\ +cB\dfrac{\tan\alpha}{\tan\beta}\cos(\beta+\varphi) + 2cB\tan\alpha\sin(\beta+\varphi) \end{Bmatrix} \tag{23}$$

By equating the resulting P_P and P_A, P_L or the limit equilibrium load sustained by the foundation can be determined according to Eq. (24):

$$p_L B\frac{\sin(\alpha-\varphi)}{\cos(\alpha-2\varphi)} = -\frac{Q_{hA}\cos(\alpha-\varphi)}{\cos(\alpha-2\varphi)} - \frac{(Q_{hP}+Q_{hQ})\cos(\beta+\varphi)}{\cos(2\varphi+\beta)} + \frac{(W_p+Q)\sin(\beta+\varphi)}{\cos(2\varphi+\beta)} - \frac{W_A\sin(\alpha-\varphi)}{\cos(\alpha-2\varphi)} + cB\begin{Bmatrix} \dfrac{\tan\alpha\cos(\beta+\varphi)}{\cos(2\varphi+\beta)} + \dfrac{2\tan\alpha\sin(\beta+\varphi)}{\cos(2\varphi+\beta)} + \\ \dfrac{\cos(\alpha-\varphi)}{\cos(\alpha-2\varphi)} + \dfrac{2\tan\alpha\sin(\alpha-\varphi)}{\cos(\alpha-2\varphi)} \end{Bmatrix} \tag{24}$$

It must be noted that the terms Q_{hA}, Q_{hP} and Q_{hQ} are replaced in Eq. (24) depending on the adopted method (conventional pseudo-dynamic, modified pseudo-dynamic or pseudo-static) and they are all previously defined in equations for each method. According to Eq. (24), p_L can be determined when the two angles α and β are known. This can be achieved by conducting an optimization process to find the angles corresponding to the most conservative p_L value. Moreover, in both conventional and modified pseudo-dynamic methods, the inertial forces imposed on the soil wedges due to earthquake are time-dependent. Therefore, in addition to the geometry, when either of the pseudo-dynamic methods is adopted, p_L has to be optimized with respect to time as well. In order to obtain individual bearing capacity factors, three separate optimization processes for each approach were carried out where each time, only one of the three parameters of c, q_f and γ would take a nonzero value to yield the most conservative estimation of the bearing capacity of the footing. Therefore, for each analysis, once p_L is determined through the process of optimization, the corresponding bearing capacity factor can be determined. In the case of a non-zero value for γ, the bearing capacity factor, N_γ can be obtained according to Eq. (25). In the case of a non-zero value for c, the bearing capacity factor, N_c can be obtained according to Eq. (26), and finally for the case of a non-zero value for q_f, the bearing capacity factor, N_q can be obtained according to Eq. (27).

$$N_\gamma = \frac{p_L}{0.5\gamma B^2} \tag{25}$$

$$N_c = \frac{p_L}{cB} \tag{26}$$

$$N_q = \frac{p_L}{q_f B} \tag{27}$$

In this study, the nonlinear optimization problem was solved using an interior-point method embedded in Matlab, MathWorks. The three bearing capacity factors are obtained for a friction angle of 30°, according to the three different pseudo-dynamic approaches, namely conventional pseudo-dynamic (CPD), spectral pseudo-dynamic (SPD) and the modified pseudo-dynamic (MPD) methods for λ/B values in the range of 0 to 40. Results are obtained and compared with each other and with the pseudo-static and static bearing capacity factors for three different horizontal acceleration coefficients (k_h) of 0.1, 0.2 and 0.3. The value of the amplification factor, f_a, has been assumed as 1 in the CPD analysis (no amplification). H has been assumed to be 10 times the foundation width, B, while the damping ratio, D, has been assumed as 5% and maintained constant throughout the analyses. In a separate series of analyses, the effect of H and D is investigated by obtaining the N_γ factor for k_h=0.1, for damping ratios of 10 and 20 % and for H assumed as 5 times the foundation width.

3 Results

Figures 3 to 11 show the variation of bearing capacity factors N_γ, N_q and N_c estimated from three different seismic approaches as elaborated earlier, with the shear wavelength λ normalized to the footing width B, for φ=30° and three different values of k_h, namely 0.1,

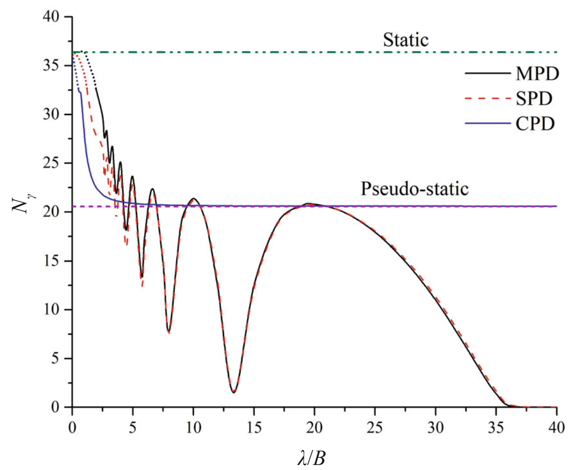

Fig. 3 Variation of N_γ with the normalized wavelength for φ=30° and k_h=0.1, H/B=10 and D=5%

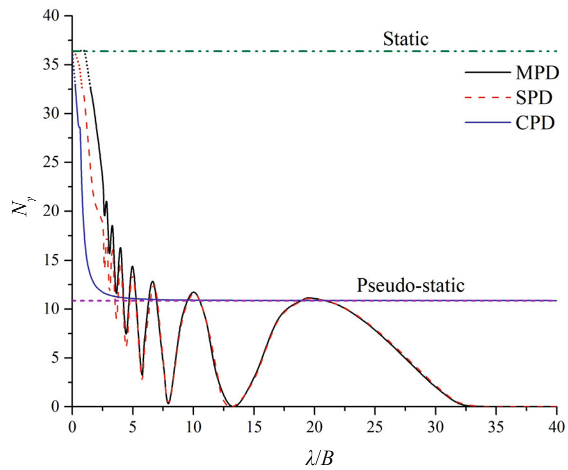

Fig. 4 Variation of N_γ with the normalized wavelength for φ=30° and k_h=0.2, H/B=10 and D=5%

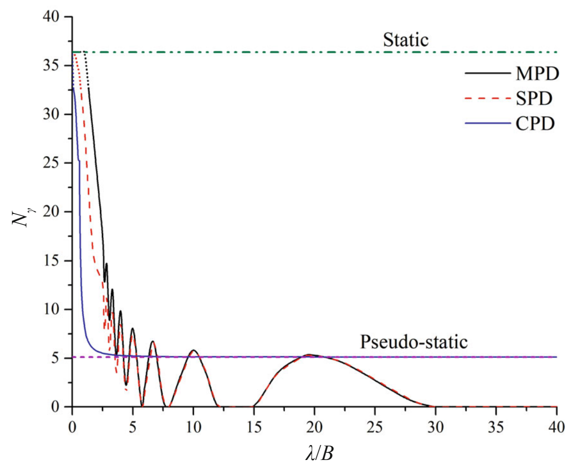

Fig. 5 Variation of N_γ with the normalized wavelength for φ=30° and k_h=0.3, H/B=10 and D=5%

0.2 and 0.3, respectively. In these analyses, H/B has been set to 10 while the damping ratio, D has been set to 5%.

Figure 12 presents the variation of the oscillation factor ξ, with depth for different wavelength ratios (λ/B) at the most critical time, obtained from the optimization process for determining the N_γ for φ=30° and k_h=0.1.

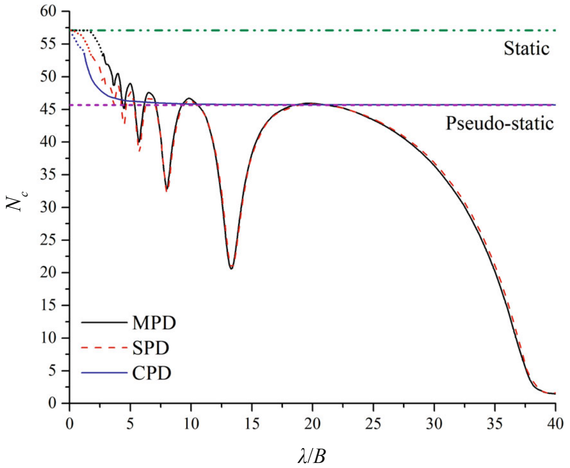

Fig. 6 Variation of N_c with the normalized wavelength for φ=30° and k_h=0.1, H/B=10 and D=5%

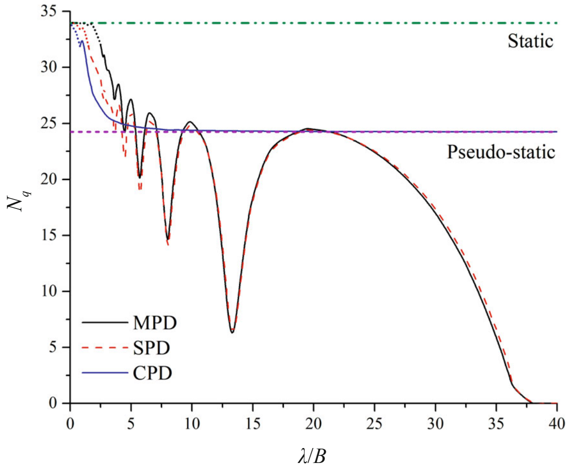

Fig. 9 Variation of N_q with the normalized wavelength for φ=30° and k_h=0.1, H/B=10 and D=5%

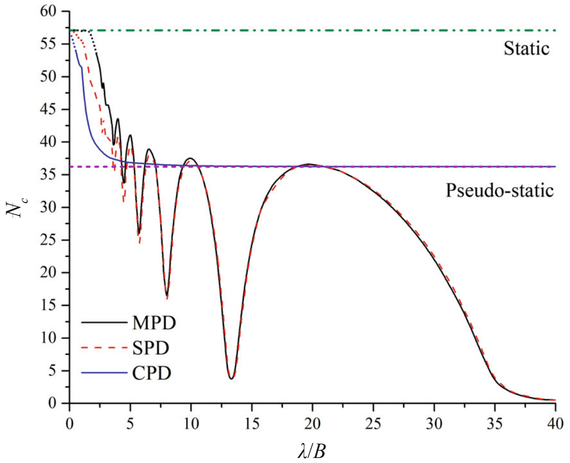

Fig. 7 Variation of N_c with the normalized wavelength for φ=30° and k_h=0.2, H/B=10 and D=5%

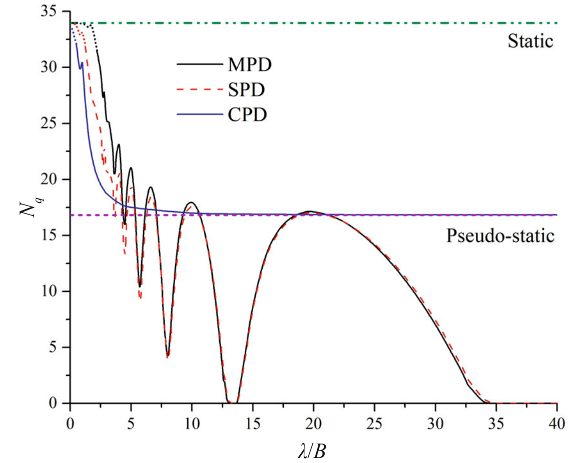

Fig. 10 Variation of N_q with the normalized wavelength for φ=30° and k_h=0.2, H/B=10 and D=5%

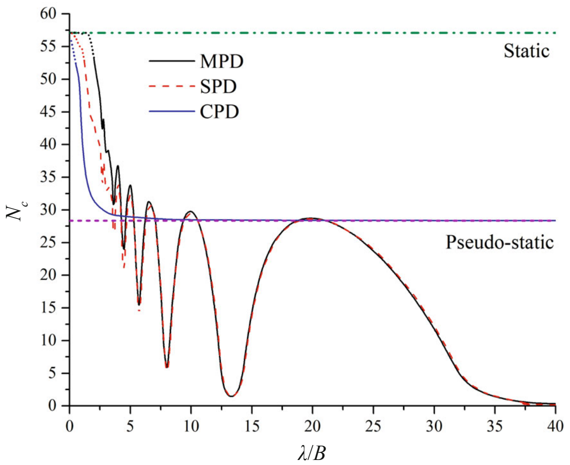

Fig. 8 Variation of N_c with the normalized wavelength for φ=30° and k_h=0.3, H/B=10 and D=5%

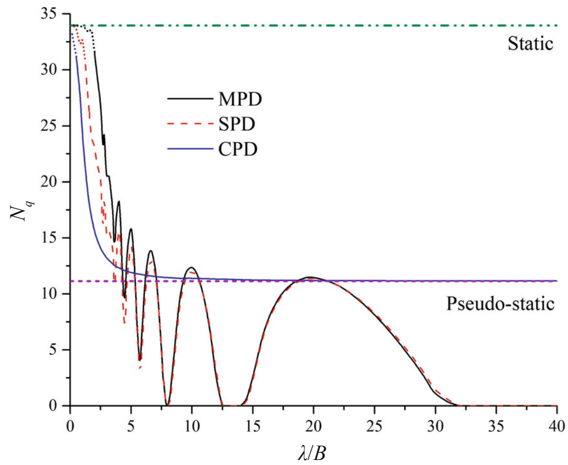

Fig. 11 Variation of N_q with the normalized wavelength for φ=30° and k_h=0.3, H/B=10 and D=5%

As seen from Figs. 3 to 11, for very small wavelengths, all three methods yield almost the same bearing capacity factors, which is close to the static bearing capacity factor. As the normalized wavelength increases, N_γ, N_q and N_c obtained from all three approaches experience a dramatic decrease. This reduction of bearing capacity with the increase in the seismic wavelength is due to the more homogenous acceleration field at higher wavelength. For smaller wavelengths, the acceleration field is a train of excitations with rapid changes in the magnitude and direction of the acceleration. As a result, a very small wavelength translates to a spatially heterogeneous acceleration field along the soil depth, where a lot of fluctuations occur in the acceleration at different depths within the failure zone, where at each point the value and direction of the acceleration can vary and different points in the soil body move at different phases from each other. The inertia forces in different directions ultimately counteract each other and the highly variable acceleration field fails to diminish the ultimate bearing capacity of the overlying shallow footing. This rapid fluctuation can be observed in Fig. 12 where the smaller the wavelength, the more spatially heterogeneous the acceleration field is and the shear wave travels many sinusoidal cycles along the stratum depth. On the other hand, for larger wavelength, the acceleration field is much more homogenous and the wave completes fewer cycles along the depth (Fig. 12). A more homogenous acceleration field in effect results in higher seismic forces applied to the soil within the failure zone, while for heterogeneous acceleration fields, due to the counteraction of the opposing inertia forces, the resulting seismic forces are minor. This will result in much higher bearing capacity values for smaller λ/B values compared to the cases with larger λ/B values, where most of the points in the influence zone move at relatively similar and in-phase accelerations. The static and pseudo-static cases are the two opposite poles of this spectrum, where the static case corresponds to an infinitely heterogeneous acceleration field and the pseudo-static case corresponds to a perfectly homogenous acceleration field, where the entire soil body experiences the same acceleration amplitude and experiences no opposing inertia forces that would otherwise arise as a result of accelerations in the opposite direction in a not perfectly homogenous case. As a result, the static case corresponds to the case of a very small wavelength while the pseudo-static case corresponds to the case of a normalized wavelength of infinity. Correspondingly, the CPD results decrease with the increase in the normalized wavelength until the results trend off towards an asymptote value which corresponds to the pseudo-static bearing capacity factor, as presented in Figs. 3 to 11. The CPD results reach their constant value at around λ/B = 5. The SPD and MPD methods present quite different trends of variation compared to the CPD method. Both the SPD and MPD methods present results slightly higher than the CPD for small λ/B values (λ/B<2.5). For this range of λ/B values, the earthquake wave has undergone attenuation, where the amplitude of the shear wave decreases as the wave travels upward. This can be corroborated by Fig. 12, where for λ/B of 0.5 and 1, the reduction in shear wave amplitude along the soil depth is clear. It can also be seen from Fig. 12 that the MPD shear wave has experienced a larger level of attenuation compared to the SPD method. This is consistent with the higher values of N_γ for MPD, seen in Fig. 3 for the aforesaid range of normalized wavelength. Similar observations can be made from the results of Figs. 4 to 11, in the aforesaid range of wavelength.

As the wavelength increases, the SPD and MPD

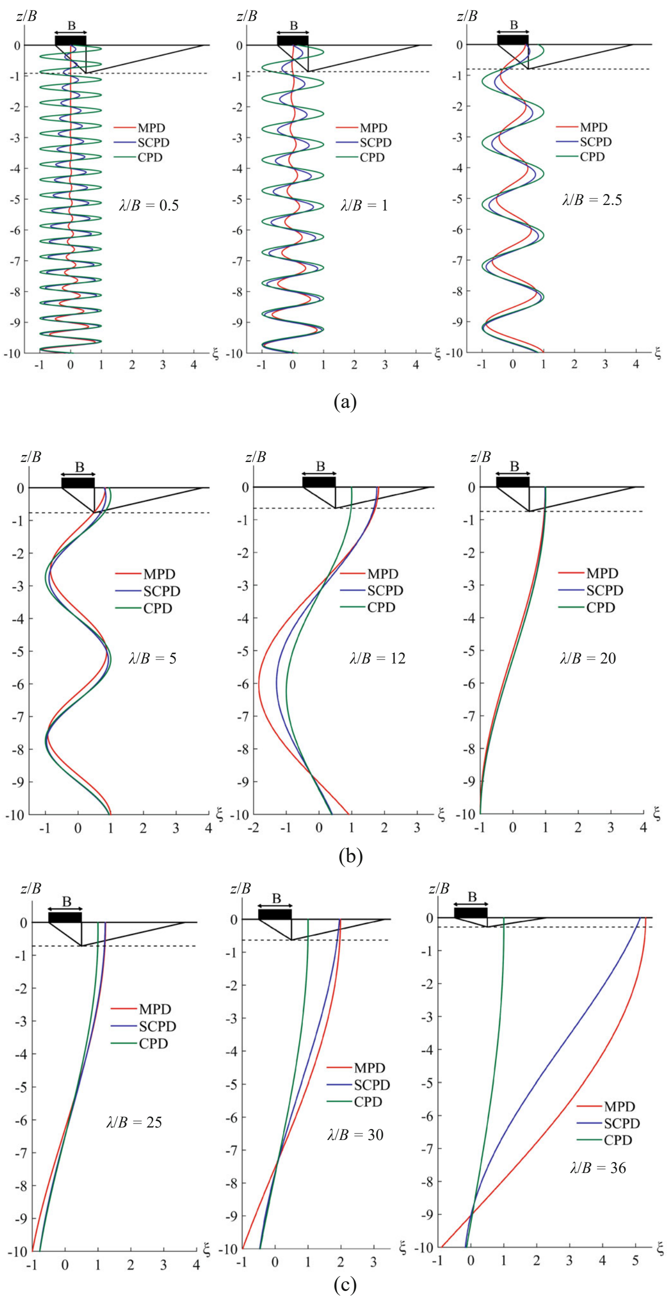

Fig. 12 Variation of the oscillation factor ξ along the soil layer depth at the critical time for different wavelengths, φ=30° and k_h=0.1, H/B=10 and D=5%

results continue to fluctuate between falling above and below the CPD values for λ/B values in the range of 5 to 10 while for λ/B values higher than 10, the SPD and MPD results fall below the CPD results due to amplification, where the wave amplitude is magnified as it travels upward. Correspondingly, in Fig. 12 various levels of amplification is observed. In addition, when λ/B equals 20, not much deviation is observed between the amplification results of the three approaches in Fig. 12, which coincide with a bearing capacity factor very close to the pseudo-static solution.

Based on the results presented in Figs. 3 to 11, it can be seen that while the CPD method manages to consider the effects of phase differences, it is unable to take into account the site effects. Site effects which arise due to the differences in sediment properties, dictate soil behavior under the effects of earthquake motion. Hence, considering site effects in seismic analysis is imperative in minimizing earthquake damage (Paudyal *et al.*, 2012 and Kanbur *et al.*, 2020).

However, the MPD and SPD methods are able to deal with both the site effects and the effects of phase differences. This can be clearly observed in Figs. 3 to 11 where in addition to the general reduction in bearing capacity with the increase of wavelength, the variation of bearing capacity with wavelength also includes successive ups and downs where with the increase in wavelength, the local maximums and minimums decrease in value. This sequential increases and reductions correspond to the variation of the amplification factor, f_a with the wavelength as presented in Fig. 13, where peaks in f_a correspond to minimums in N_γ and vice versa. The local peaks in f_a occur at wavelengths that correspond to the natural frequencies of the soil. These frequencies are presented in Eq. (28) and the corresponding normalized wavelengths are presented in Eq. (29).

$$f = \left(\frac{1}{4} + \frac{n}{2}\right) \times \frac{V_s}{H} \qquad n = 0,\ 1,\ 2,\ ...,\ \infty \tag{28}$$

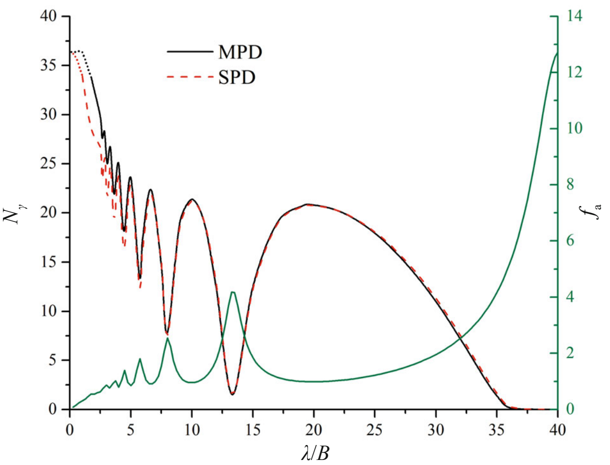

Fig. 13 Variation of N_γ with the normalized wavelength for φ=30° and k_h=0.2, H/B=10 and D=5% superimposed with the variation of f_a with the normalized wavelength

where f is the soil natural frequency.

$$\lambda / H = \frac{1}{\left(\frac{1}{4} + \frac{n}{2}\right)} \qquad n = 0,\ 1,\ 2,\ ...,\ \infty \tag{29}$$

Based on these results, the MPD and SPD methods both present fairly consistent results and are able to deal with both the site effects and the effects of phase differences. Contrary to the CPD method which relies on an a priori value of f_a to implement the potential amplifications of ground motion, the MPD and SPD methods are able to take account of the effects of soil′s properties, including its damping properties and its shear wave velocity, as well as the geometry of the site (thickness of the layer) on the amplification of the base ground motion.

Figures 14 and 15 illustrate the variation of the amplitude of the oscillation factor for the SPD and MPD methods, respectively. The acceleration transfer function curve, previously presented in Fig. 13 can also be seen in Figs. 14 and 15 in the z/H=0 plane. It can be seen that while the SPD approach assumes a linearly depth-varying oscillation amplitude, according to the MPD method the ξ amplitude follows a harmonic trend of variation with the soil depth. Despite the different amplitude profiles between the SPD and MPD seismic formulations, the resulting bearing capacity values are quite similar, because they are both apt to capture the site effects and the out-of-phase behavior of seismic waves in the soil stratum underneath. The linear formulation of the SPD turns this approach into a simpler alternative to the MPD method that can be quite useful in solving stability problems, where complex failure mechanisms are employed and an integration has to be carried out over the depth of the soil.

In order to examine the consistency of the SPD and MPD approaches for different damping ratios, N_γ values were obtained for φ=30°, k_h=0.1, H/B=10 and two different damping ratios of 10% and 20%. Figures 16 and 17 show the variation of the N_γ as estimated from the three different seismic approaches, with λ/B. As seen from the figures, the same general trend of reduction with the increase in λ/B occurs. However, it is clear that the increase in damping ratio has led to an increase in N_γ, as can be expected. In addition, while the MPD and SPD approaches are still quite consistent with one another, a higher level of inconsistency is observed at higher damping ratios.

Finally, the consistency of the SPD and MPD approaches for different bedrock depths was examined by obtaining N_γ values for φ=30°, k_h=0.1, D=5% and H/B=5. Figure 18 shows the variation of the N_γ as estimated from the three different seismic approaches with λ/B. It can be seen from the figure that the MPD and SPD approaches remain consistent.

Based on the results provided, it can be concluded that while the CPD method is not able to take into account the site and damping effects, the MPD and SPD approaches make use of formulations that embed the aforesaid effects in the bearing capacity problem. Both SPD and MPD methods are able to take account of the dependence of the amplification of the base motion on the soil′s shear wave velocity, V_s, thickness of the soil layer, H and soil damping ratio, D. In addition, both methods present quite similar results. Therefore, instead of assuming an a priori f_a value in the CPD approach, by entering the amplification factor as a function of the non-dimensional frequency and damping ratio, the CPD method can be upgraded to a spectral analysis level (SPD), whose results fare well against those of the MPD method.

In the next section, an example is provided to demonstrate the effectiveness of the methods in practice.

Example: A footing of width equal to 3 m is to be placed over a soil stratum with a depth of 30 m above the rigid bedrock. The soil has an average shear wave velocity of 180 m/s, a unit weight of 19 kN/m^3 and a damping ratio of 5%. Soil friction angle is equal to 30°, cohesion is null and the footing is placed at a depth of 1 m into the soil. Considering a bedrock acceleration of 0.3 g with a frequency of 4 Hz, what is the bearing capacity of the footing according to the PS, CPD, SPD and MPD approaches?

Since the pseudo-static analysis is not a spectral analysis, the soil shear wave velocity and damping have no bearing on the result. On the other hand, for the spectral analysis:

$$\lambda / B = V_s / (f \times B) = 180 / (4 \times 3) = 15$$

N_γ and N_q for k_h=0.3 according to PS, CPD (f_a=1), SPD and MPD methods are obtained from Figs. 5 and 11 and are presented in Table 1 along with the resulting ultimate bearing capacity, q_u. As an example, the PS bearing capacity is found according to the following formula.

$$q_u = cN_c + qN_q + \frac{1}{2}\gamma BN_\gamma$$
$$= 1 \times 19 \times 11.14 + \frac{1}{2} \times 19 \times 3 \times 5.12 = 357.58 \text{ kN/m}^2$$

As seen from the table, the q_u obtained from SPD and MPD methods are consistent with one another. However, a significant disparity exists between the CPD/PS and SPD/MPD results. This is due to the

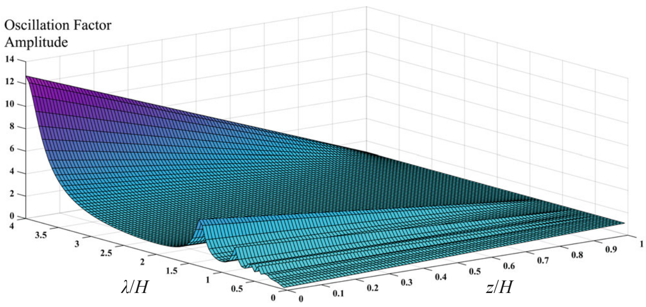

Fig. 14 Variation of the oscillation factor amplitude with the normalized wavelength and layer depth for the SPD method

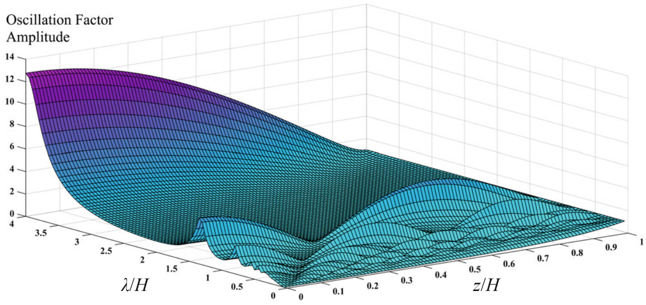

Fig. 15 Variation of the oscillation factor amplitude with the normalized wavelength and layer depth for the MPD method

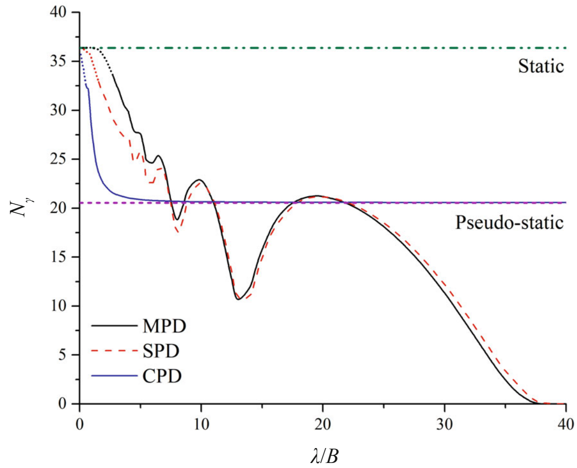

Fig. 16 Variation of N_γ with the normalized wavelength for φ=30° and k_h=0.1, H/B=10 and D=10%

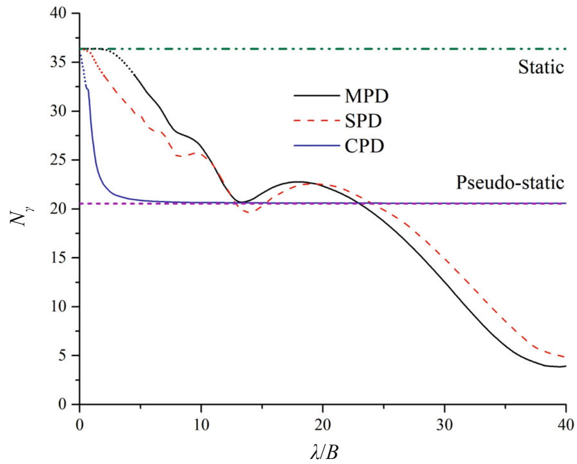

Fig. 17 Variation of N_γ with the normalized wavelength for φ=30° and k_h=0.1, H/B=10 and D=20%

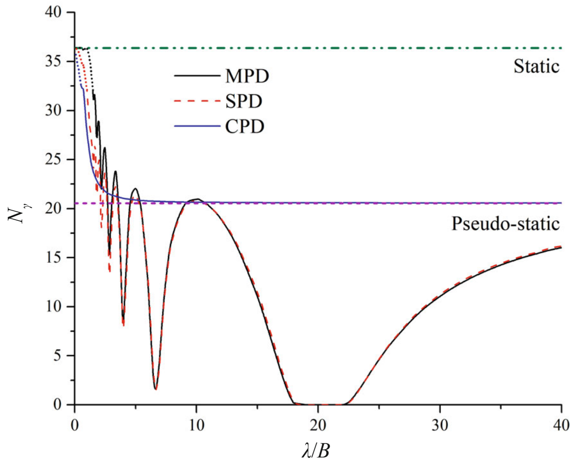

Fig. 18 Variation of N_γ with the normalized wavelength for φ=30° and k_h=0.1, H/B=5 and D=5%

Table 1 Ultimate bearing capacity according to different seismic approaches

Method	N_γ	N_q	q_u (kN/m^2)
PS	5.12	11.14	357.58
CPD	5.13	11.23	359.58
SPD	0.07	2.32	46.08
MPD	0.13	2.58	52.73

significant amplification that the shear wave experiences as demonstrated according to the following equation:

$$f_a = \frac{1}{\sqrt{\cos^2(2\pi(H/\lambda)) + (2\pi D(H/\lambda))^2}}$$
$$= \frac{1}{\sqrt{\cos^2(2\pi\times(50/75)) + (2\pi\times 0.05\times(50/75))^2}} = 1.84$$

The PS and CPD method fail to consider this amplification and that leads to a significant overestimation of bearing capacity.

4 Conclusions

The conventional and modified pseudo-dynamic approaches are employed to carry out seismic bearing capacity analyses of strip foundations, using the limit equilibrium method with a two-wedge failure mechanism. In addition, a spectral version of the conventional pseudo-dynamic method was also utilized by considering the amplification factor to be a function of the non-dimensional frequency and the soil damping ratio.

Based on the results, the CPD method with f_a=1, presents N_γ values that start out from the static value at a λ/B of zero, and eventually trend off towards the pseudo-static N_γ as λ/B approaches λ/B = 5. The reduction in wavelength was shown to result in a more spatially heterogenous acceleration field and the shear waves were observed to complete more cycles as they travel up through the soil. This heterogeneity alleviates some of the seismic inertia forces on the soil body due to the counteraction of the opposing inertia forces, leading to higher bearing capacity values.

SPD and MPD bearing capacity results were observed to experience the same general reduction in bearing capacity with the increase of wavelength. However, the SPD and MPD bearing capacity results also included successive ups and downs corresponding to the soil's natural frequencies, where the local maximums and minimums decrease in value as the wavelength increases. For λ/B<2.5, SPD and MPD results were slightly higher than those of the CPD which was consistent with attenuation of the shear wave, with MPD results indicative of a higher level of attenuation. For 5<λ/B<10, SPD and MPD results fluctuate between falling above and below the CPD values. For 10<λ/B, SPD and MPD results fall below the CPD results, demonstrating amplification.

While according to the MPD method the oscillation amplitude follows a harmonic trend of variation with the soil depth, the SPD approach assumes a linearly depth-varying oscillation amplitude. Therefore, the SPD formulations are simpler and easier to apply. Despite the different amplitude profiles between the SPD and MPD seismic formulations, the resulting bearing capacity values are quite similar and both methods are shown to be apt to capture the site effects and the out-of-phase behavior of seismic waves in the soil stratum underneath. With the increase in damping ratio, a higher level of inconsistency was observed between the MPD and SPD results, despite them remaining generally consistent.

Based on the results, the MPD and SPD methods are capable of taking into account damping and site effects and they produce results consistent with one another. Consequently, including an amplification factor that is a function of the non-dimensional frequency and damping ratio, into the CPD formulation can enhance its efficacy to compete well with the MPD method in bearing capacity analyses, while still remaining simple and easy to apply, due to its linear formulation.

References

Ahmad SM and Choudhury D (2008a), "Pseudo-Dynamic Approach of Seismic Design for Waterfront Reinforced Soil-Wall," *Geotextiles and Geomembranes,* 26(4): 291–301.

Ahmad SM and Choudhury D (2008b), "Stability of Waterfront Retaining Wall Subjected to Pseudo-

Dynamic Earthquake Forces and Tsunami," *Journal of Earthquake and Tsunami*, **2**(2): 107–131.

Ahmad SM and Choudhury D (2010), "Seismic Rotational Stability of Waterfront Retaining Wall Using Pseudodynamic Method," *International Journal of Geomechanics*, **10**(1): 45–52.

Azad A, Yasrobi SS and Pak A (2008), "Seismic Active Pressure Distribution History Behind Rigid Retaining Walls," *Soil Dynamics and Earthquake Engineering*, **28**(5): 365–375.

Basha BM and Babu GS (2009a), "Computation of Sliding Displacements of Bridge Abutments by Pseudo-Dynamic Method," *Soil Dynamics and Earthquake Engineering*, **29**(1): 103–120.

Basha BM and Babu GS (2009b), "Seismic Reliability Assessment of External Stability of Reinforced Soil Walls Using Pseudo-Dynamic Method," *Geosynthetics International*, **16**(3): 197–215.

Basha BM and Babu GS (2010), "Seismic Rotational Displacements of Gravity Walls by Pseudodynamic Method with Curved Rupture Surface," *International Journal of Geomechanics*, **10**(3): 93–105.

Basha BM and Babu GS (2011), "Seismic Reliability Assessment of Internal Stability of Reinforced Soil Walls Using the Pseudo-Dynamic Method," *Geosynthetics International*, **18**(5): 221–241.

Bellezza I (2014), "A New Pseudo-Dynamic Approach for Seismic Active Soil Thrust," *Geotechnical and Geological Engineering*, **32**(2): 561–576.

Bellezza I (2015), "Seismic Active Earth Pressure on Walls Using a New Pseudo-Dynamic Approach," *Geotechnical and Geological Engineering*, **33**(4): 795–812.

Bellezza I, D'Alberto D and Fentini R (2012), "Pseudo-Dynamic Approach for Active Thrust of Submerged Soils," *Proceedings of the Institution of Civil Engineers-Geotechnical Engineering*, **165**(5): 321–333.

Chakraborty D and Choudhury D (2014a), "Stability of Non-Vertical Waterfront Retaining Wall Supporting Inclined Backfill Under Earthquake and Tsunami," *Ocean Engineering*, **78**: 1–10.

Chakraborty D and Choudhury D (2014b), "Sliding Stability of Non-Vertical Waterfront Retaining Wall Supporting Inclined Backfill Subjected to Pseudo-Dynamic Earthquake Forces," *Applied Ocean Research*, **47**: 174–182.

Cheng YN, Sun S and Ruan X (2013), "Pseudo-Dynamic Analysis of Seismic Stability of Reinforced Soil Walls," *Rock and Soil Mechanics*, **34**(12): 3573–3579.

Choudhury D and Ahmad SM (2008), "Stability of Waterfront Retaining Wall Subjected to Pseudodynamic Earthquake Forces," *Journal of Waterway, Port, Coastal and Ocean Engineering*, **134**(4): 252–260.

Choudhury D, Katdare AD and Pain A (2014), "New Method to Compute Seismic Active Earth Pressure on Retaining Wall Considering Seismic Waves," *Geotechnical and Geological Engineering*, **32**(2): 391–402.

Choudhury D and Nimbalkar SS (2005), "Seismic Passive Resistance by Pseudo-Dynamic Method," *Géotechnique*, **55**(9): 699–702.

Choudhury D and Nimbalkar SS (2006), "Pseudo-Dynamic Approach of Seismic Active Earth Pressure Behind Retaining Wall," *Geotechnical and Geological Engineering*, **24**(5): 1103–1113.

Choudhury D and Nimbalkar SS (2007), "Seismic Rotational Displacement of Gravity Walls by Pseudo-Dynamic Method: Passive Case," *Soil Dynamics and Earthquake Engineering*, **27**(3): 242–249.

Choudhury D and Nimbalkar SS (2008), "Seismic Rotational Displacement of Gravity Walls by Pseudodynamic Method," *International Journal of Geomechanics*, **8**(3): 169–175.

Choudhury D, Nimbalkar SS and Mandal JN (2007), "External Stability of Reinforced Soil Walls Under Seismic Conditions," *Geosynthetics International*, **14**(4): 211–218.

Eskandarinejad A and Shafiee AH (2011), "Pseudo-Dynamic Analysis of Seismic Stability of Reinforced Slopes Considering Non-associated Flow Rule," *Journal of Central South University of Technology*, **18**(6): 2091–2099.

Fathipour H, Payan M, Jamshidi Chenari R and Senetakis K (2021a), "Limit Analysis of Modified Pseudo-Dynamic Lateral Earth Pressures for Backfill Soil with Depth-Varying Damping Characteristics Using FEM-Second Order Cone Programming," *International Journal for Numerical and Analytical Methods in Geomechanics*, **21**(2): 04020258.

Fathipour H, Safardoost Siahmazgi AH, Payan M, Veiskarami M and Jamshidi Chenari R (2021b), "Limit Analysis of Modified Pseudodynamic Lateral Earth Pressure in Anisotropic Frictional Medium Using Finite-Element and Second-Order Cone Programming," *International Journal of Geomechanics*, DOI: 10.1002/nag.3269.

Ghanbari A and Ahmadabadi M (2010), "Pseudo-Dynamic Active Earth Pressure Analysis of Inclined Retaining Walls Using Horizontal Slices Method," *Scientia Iranica. Transaction A, Civil Engineering*, **17**(2): 118–130.

Ghosh P (2007), "Seismic Passive Earth Pressure Behind Non-Vertical Retaining Wall Using Pseudo-Dynamic Analysis," *Geotechnical and Geological Engineering*, **25**(6): 693–703.

Ghosh P (2008a), "Seismic Active Earth Pressure Behind a Nonvertical Retaining Wall Using Pseudo-Dynamic Analysis," *Canadian Geotechnical Journal*, **45**(1): 117–123.

Ghosh P (2008b), "Upper Bound Solutions of Bearing Capacity of Strip Footing by Pseudo-Dynamic Approach," *Acta Geotechnica*, **3**(2): 115–123.

Ghosh P and Choudhury D (2011), "Seismic Bearing Capacity Factors for Shallow Strip Footings by Pseudodynamic Approach," *Disaster Advances*, **4**(3): 34–42.

Ghosh P and Kolathayar S (2011), "Seismic Passive Earth Pressure Behind Non Vertical Wall with Composite Failure Mechanism: Pseudo-Dynamic Approach," *Geotechnical and Geological Engineering*, **29**(3): 363–373.

Ghosh S (2010), "Pseudo-Dynamic Active Force and Pressure Behind Battered Retaining Wall Supporting Inclined Backfill," *Soil Dynamics and Earthquake Engineering*, **30**(11): 1226–1232.

Ghosh S and Debnath L (2017), "Seismic Bearing Capacity of Shallow Strip Footing with Coulomb Failure Mechanism Using Limit Equilibrium Method," *Geotechnical and Geological Engineering*, **35**(6): 2647–2661.

Ghosh S and Saha A (2014), "Nonlinear Failure Surface and Pseudodynamic Passive Resistance of a Battered-Faced Retaining Wall Supporting *c*-*φ* Backfill," *International Journal of Geomechanics*, **14**(3): 04014010-1–9.

Ghosh S and Sharma RP (2012), "Pseudo-Dynamic Evaluation of Passive Response on the Back of a Retaining Wall Supporting c-Φ Backfill," *Geomechanics and Geoengineering*, **7**(2): 115–121.

Izadi A, Nazemi Sabet Soumehsaraei M, Jamshidi Chenari R, Moallemi S and Javankhoshdel S (2019), "Spectral Bearing Capacity Analysis of Strip Footings Under Pseudo-Dynamic Excitation," *Geomechanics and Geoengineering*, 1–20.

Jamshidi Chenari R and Aminzadeh Bostani Taleshani S (2016), "Site Response of Heterogeneous Natural Deposits to Harmonic Excitation Applied to More than 100 Case Histories," *Earthquake Engineering and Engineering Vibration*, **15**(2): 341–356.

Kanbur MZ, Silahtar A and Aktan G (2020), "Local Site Effects Evaluation by Surface Wave and H/V Survey Methods in Senirkent (Isparta) Region, Southwestern Turkey," *Earthquake Engineering and Engineering Vibration*, **19**(2): 321–333.

Kazemi Esfeh P, Nadi B and Fantuzzi N (2020), "Influence of Random Heterogeneity of Shear Wave Velocity on Sliding Mass Response and Seismic Deformations of Earth Slopes," *Earthquake Engineering and Engineering Vibration*, **19**(2): 269–287.

Khatri VN (2019), "Determination of Passive Earth Pressure with Lower Bound Finite Elements Limit Analysis and Modified Pseudo-Dynamic Method," *Geomechanics and Geoengineering*, **14**(3): 218–229.

Kramer S (1996), *Geotechnical Earthquake Engineering*, Prentice Hall, Inc., Englewood Cliffs, N.J.

Kurup SS and Kolathayar S (2018), "Seismic Bearing Capacity Factor Considering Composite Failure Mechanism: Pseudo-Dynamic Approach," *International Journal of Geotechnical Earthquake Engineering*, **9**(1): 65–77.

Nadgouda K and Choudhury D (2019), "Seismic Bearing Capacity Factor $N_{\gamma e}$ for Dry Sand Beneath Strip Footing Using Modified Pseudo-Dynamic Method with Composite Failure Surface," *International Journal of Geotechnical Engineering*, 1–10.

Narasimha Reddy GV, Choudhury D, Madhav MR and Saibaba Reddy E (2009), "Pseudo-Dynamic Analysis of Reinforced Soil Wall Subjected to Oblique Displacement," *Geosynthetics International*, **16**(2): 61–70.

Nimbalkar SS and Choudhury D (2007), "Sliding Stability and Seismic Design of Retaining Wall by Pseudo-Dynamic Method for Passive Case," *Soil Dynamics and Earthquake Engineering*, **27**(6): 497–505.

Nimbalkar SS and Choudhury D (2008), "Effects of Body Waves and Soil Amplification on Seismic Earth Pressures," *Journal of Earthquake and Tsunami*, **2**(1): 33–52.

Nimbalkar SS, Choudhury D and Mandal JN (2006), "Seismic Stability of Reinforced-Soil Wall by Pseudo-Dynamic Method," *Geosynthetics International*, **13**(3): 111–119.

Pain A, Choudhury D and Bhattacharyya SK (2015), "Seismic Stability of Retaining Wall–Soil Sliding Interaction Using Modified Pseudo-Dynamic Method," *Géotechnique Letters*, **5**(1): 56–61.

Pain A, Choudhury D and Bhattacharyya SK (2016a), "Seismic Uplift Capacity of Horizontal Strip Anchors Using a Modified Pseudodynamic Approach," *International Journal of Geomechanics*, **16**(1): 04015025-1–12.

Pain A, Choudhury D and Bhattacharyya SK (2016b), "The Seismic Bearing Capacity Factor for Surface Strip Footings," *Geo-Chicago*, 197–206.

Pain A, Choudhury D and Bhattacharyya SK (2017a), "Seismic Passive Earth Resistance Using Modified Pseudo-Dynamic Method," *Earthquake Engineering and Engineering Vibration*, **16**(2): 263–274.

Pain A, Choudhury D and Bhattacharyya SK (2017b), "Seismic Rotational Stability of Gravity Retaining Walls by Modified Pseudo-Dynamic Method," *Soil Dynamics and Earthquake Engineering*, **94**: 244–253.

Paudyal YR, Yatabe R, Bhandary NP and Dahal RK (2012), "A Study of Local Amplification Effect of Soil Layers on Ground Motion in the Kathmandu Valley Using Microtremor Analysis," *Earthquake Engineering and Engineering Vibration*, **11**(2): 257–268.

Prandtl L (1921), "Uber die Eindringungstestigkeit Plastisher Baustoffe und die Festigkeit von Schneiden," *Zeitschrift Für Angewandt Mathematik Und Mechanik,* **1**(1): 15–30.

Qin CB and Chian SC (2018), "Kinematic Analysis of Seismic Slope Stability with a Discretisation

Technique and Pseudo-Dynamic Approach: A New Perspective," *Géotechnique*, **68**(6): 492–503.

Rajesh BG and Choudhury D (2017a), "Generalized Seismic Active Thrust on a Retaining Wall with Submerged Backfill Using a Modified Pseudodynamic Method," *International Journal of Geomechanics*, **17**(3): 06016023-1–2.

Rajesh BG and Choudhury D (2017b), "Seismic Passive Earth Resistance in Submerged Soils Using Modified Pseudo-Dynamic Method with Curved Rupture Surface," *Marine Georesources and Geotechnology*, **35**(7): 930–938.

Richards Jr R, Elms DG and Budhu M (1993), "Seismic Bearing Capacity and Settlements of Foundations," *Journal of Geotechnical Engineering*, **119**(4): 662–674.

Ruan XB, Cheng Q and Sun S (2013a), "Active Seismic Pressure Against Retaining Wall Backfilled with Cohesive Soils," *Soil Mechanics and Foundations and Engineering,* **50**(3): 116–122.

Ruan XB, Lin K, Han X and Zhu D (2018), "Required Reinforcement Length for External Stability of MSE Walls Using Pseudo-Dynamic Method," *GeoShanghai International Conference*, Springer, Singapore, 153–160.

Ruan XB and Sun SL (2013), "Seismic Stability of Reinforced Soil Walls Under Bearing Capacity Failure by Pseudo-Dynamic Method," *Journal of Central South University*, **20**(9): 2593–2598.

Ruan XB, Sun SL and Liu WL (2013), "Effect of the Amplification Factor on Seismic Stability of Expanded Municipal Solid Waste Landfills Using the Pseudo-Dynamic Method," *Journal of Zhejiang University Science A*, **14**(10): 731–738.

Ruan XB, Yu R and Sun S (2012), "Analysis of Seismic Active Earth Pressure on Retaining Wall Based on Pseudo-Dynamic Method," *Journal of Highway Transportation and Research Development*, **29**(8): 25–30.

Safardoost Siahmazgi AH, Fathipour H, Jamshidi Chenari R, Veiskarami M and Payan M (2021), "Evaluation of the Pseudo-Dynamic Bearing Capacity of Surface Footings on Cohesionless Soils Using Finite Element Lower Bound Limit Analysis," *Geomechanics and Geoengineering*, 1–13.

Saha A and Ghosh S (2015a), "Pseudo-Dynamic Analysis for Bearing Capacity of Foundation Resting on c–Φ Soil," *International Journal of Geotechnical Engineering*, **9**(4): 379–387.

Saha A and Ghosh S (2015b), "Pseudo-Dynamic Bearing Capacity of Shallow Strip Footing Resting on c-Φ Soil Considering Composite Failure Surface: Bearing Capacity Analysis Using Pseudo-Dynamic Method," *International Journal of Geotechnical Earthquake Engineering*, **6**(2): 12–34.

Saha A and Ghosh S (2017), "Modified Pseudo-Dynamic Bearing Capacity Analysis of Shallow Strip Footing Considering Total Seismic Wave," *International Journal of Geotechnical Engineering*, **14**(1): 101–109.

Saha A and Ghosh S (2020), "Modified Pseudo-Dynamic Bearing Capacity of Shallow Strip Footing Considering Fully Log-Spiral Passive Zone with Global Center," *Iranian Journal of Science and Technology, Transactions of Civil Engineering*, **44**: 683–693.

Saha A, Saha AK and Ghosh S (2018), "Pseudodynamic Bearing Capacity Analysis of Shallow Strip Footing Using the Advanced Optimization Technique 'Hybrid Symbiosis Organisms Search Algorithm' with Numerical Validation," *Advances in Civil Engineering*, **1**: 1–18.

Sarangi P and Ghosh P (2016), "Seismic Analysis of Nailed Vertical Excavation Using Pseudo-Dynamic Approach," *Earthquake Engineering and Engineering Vibration*, **15**(4): 621–631.

Shafiee AH, Eskandarinejad A and Jahanandish M (2010), "Seismic Passive Earth Thrust on Retaining Walls with Cohesive Backfills Using Pseudo-Dynamic Approach," *Geotechnical and Geological Engineering*, **28**(4): 525–531.

Shekarian S and Ghanbari A (2008), "A Pseudo-Dynamic Method to Analyze Retaining Wall with Reinforced and Unreinforced Backfill," *Journal of Seismology and Earthquake Engineering*, **10**(1): 41–47.

Shekarian S, Ghanbari A and Farhadi A (2008), "New Seismic Parameters in the Analysis of Retaining Walls with Reinforced Backfill," *Geotextiles and Geomembranes*, **26**(4): 350–356.

Steedman RS and Zeng X (1990), "The Influence of Phase on the Calculation of Pseudo-Static Earth Pressure on a Retaining Wall," *Géotechnique*, **40**(1): 103–112.

Wang KH, Ma SJ and Wu WB (2011), "Pseudo-Dynamic Analysis of Overturning Stability of Retaining Wall," *Journal of Central South University of Technology*, **18**(6): 2085–2090.

Zhou XP, Gu XB, Yu MH and Qian QH (2016), "Seismic Bearing Capacity of Shallow Foundations Resting on Rock Masses Subjected to Seismic Loads," *KSCE Journal of Civil Engineering*, **20**(1): 216–228.

Zhou XP, Qian Q, Cheng H and Zhang H (2015), "Stability Analysis of Two-dimensional Landslides Subjected to Seismic Loads," *Acta Mechanica Solida Sinica*, **28**(3): 262–276.